Tellus (1995), 47A, 145–161
Printed in Belgium – all rights reserved

TELLUS
ISSN 0280–6495

Low-order models, initialization, and the slow manifold

By JAMES H. CURRY, SUE ELLEN HAUPT* and MARTHA NESBITT LIMBER, *Program in Applied Mathematics, The University of Colorado, Boulder, CO 80309, USA*

(Manuscript received 15 October 1992; in final form 14 April 1994)

ABSTRACT

A nine equation low-order model of the shallow water equations is used as a testbed to compare several initialization strategies and to find points satisfying conditions of "slowness." Several methods are explored to initialize the low order model: (1) Lorenz's method of successively zeroing tendencies; (2) minimization of the sum of the squares of the tendencies; (3) use of a balance condition. We find that the balance condition produces the smoothest solution on a consistent basis. In addition, Lorenz initialization, the Newton-Kantorovich Theorem, and the Nested Interval Property are used to compute points devoid of gravity waves to order N for low values of the forcing ($F_1 \leqslant 0.1$). Several of these points are calculated.

1. Introduction

Numerical weather prediction practitioners have long recognized the need to use filtered data to initialize their time integrations. The initialization strategy is often necessary to avoid spurious gravity waves which may be of sufficient amplitude to mask physical phenomena of interest, or cause serious problems with the assimilation of observations, or occasionally lead to numerical instability in the model. Although a certain amount of gravity wave activity is natural in any model (as is true in the real atmosphere), merely filtering out the fast gravitational modes upon initialization is frequently inadequate because they are typically quickly regenerated through the model's nonlinear interactions between the lower frequency rotational (also known as quasigeostrophic, Rossby, or slow) modes after a short time. Instead, most methods attempt to determine a balance, to set time tendencies of the gravity modes to zero or to make them small, or use some other filtering strategy. Current operational models use a form of nonlinear normal mode initialization pioneered in the late 1970's by Machenhauer (1977) and Baer and Tribbia (1977). For a thorough review of the history, description of the methodology, and insights into the relationship to other aspects of the model, see Daley (1991), Errico (1989), or Daley (1981).

The initialization process effectively defines a "manifold." An example of a manifold which may be useful to bear in mind is the graph of a function. In this example, associated with each independent variable, x, is at most one other variable, y, and the relationship $y = f(x)$ is obtained. Such a graph of a function is a manifold, but the equation $x^2 + y^2 = 1$ does not define a manifold because for each x value there are two possible y values, depending on sign. There is a growing body of material which suggests that much of the long term behavior of a dynamical system often occurs in a small portion of the available phase space and is restricted to local manifolds. In some cases, when models have both forcing and dissipation, and when the dissipation is strong enough to ensure that solutions of the model equations remain bounded but the forcing is sufficiently strong to guarantee that the solutions behave in an "interesting" manner, it is possible to establish rigorously that manifolds, termed *inertial manifolds*, exist and absorb all solution curves.

When initialization successfully produces initial

* Corresponding author.

states for which the time tendencies of the gravity modes are as desired, these states may lie on a manifold. That is, while a functional relationship has been established between initial states and states where the time tendency of the gravity modes satisfy some criterion, some neighboring points must also satisfy the criterion. If such a manifold contains subsequent states under evolution, then it is termed an *invariant* manifold. If evolution along this manifold is devoid of gravity wave activity, it is the *slow manifold* (Leith, 1980). Projection onto the slow manifold might possibly require a *superbalance condition* (Lorenz, 1980) which would be the "perfect" initialization of a model.

In the past decade, there has been considerable debate as to whether the slow manifold actually exists. A common approach to the problem has been to study low-order models (LOMs), that is, truncated systems containing a few variables rather than the full partial differential equations. Lorenz (1960, 1982) argued that much can be learned about the behavior of more realistic systems through the understanding of these simplified models. To address questions of initialization, Lorenz (1980) used a 9-variable model as an analogue to the Primitive Equations (PE). This model was further analyzed by Gent and McWilliams (1982), Kopell (1985), Vautard and Legras (1986), Warn and Menard (1986), Lorenz (1986), Curry and Winsand (1986), and Vallis (1992), among others. Subsequently, Lorenz (1986) compressed the 1980 model to five variables and studied it further (Lorenz and Krishnamurthy, 1987). For this reduced system Jacobs (1991) proved that a slow manifold exists (at least locally) by using the Hartman–Grobman theorem (Guckenheimer and Holmes, 1983) and a power series expansion: such manifolds are analytic but not all manifolds will enjoy this property. Jacobs also showed that the manifold is stable and can be constructed in the neighborhood of a known stationary solution of the equation. Lorenz (1992) questioned whether evolution from the neighborhood of such a stationary point remains "slow" for all time. Recent work (Camassa, 1994; Boyd, 1994b) suggests that no globally invariant manifold can exist for this five equation model. Boyd (1994a) has pointed out that the meaning of "slow" is not necessarily the same in each of the above articles. In this present study, by *slow* we mean a state of the system where the time scales are sufficiently separated and the fast gravity modes are effectively eliminated.

Developing along a somewhat related course has been the study of intermediate models. A thorough study of intermediate balanced equations, their relationship to the PE, and their regimes of validity has been done by McWilliams and Gent (1980); Gent and McWilliams (1982), (1983a, b); Norton et al. (1986); McWilliams et al. (1986); McWilliams et al. (1990); Allen et al. (1990a, b); and Barth et al. (1990). A possible philosophical ansatz is that the "ideal" intermediate model ought to project onto the slow manifold. Intermediate models have also been developed for the 9-variable truncated system of Lorenz (1980) by Gent and McWilliams (1982) and are discussed in Section 2.

This current study focuses on the problems of initialization and the existence of a slow manifold for the 9-variable model of Lorenz (1980) (Section 2). In analogy with the thinking of Lorenz, we believe that defining the best initialization strategies for such LOM's will produce useful information on initialization of full PDEs. Various initialization schemes are explored in Section 3 where the goal is to produce an integration of the low order PE with minimal or no gravity wave activity. Some success is achieved for modest forcing. One of the better initialization techniques is to simply use the initial data from the truncated BE model in the PE model. In Section 4, we comment on the model bifurcations and the implications for the topology of the attractor. Then we use a proof strategy coupled with numerical computations to find several slow points for low values of the forcing. Our findings strongly suggest that exact computations are intractable using any standard computational approach to the problem. Results are summarized and discussed in Section 5. For another approach to the issues involving initialization, manifolds and balance equations see Vallis (1992) or Kopell (1985).

2. The low-order models

The model system of equations studied here is the 9-variable truncated Primitive Equation (PE) system introduced by Lorenz (1980).

The model is derived from the shallow water equations governing hydrostatic, homogeneous, incompressible flow on an infinite f-plane moving over topography.

$$\left(\frac{\partial}{\partial t}+\boldsymbol{V}\cdot\nabla\right)\boldsymbol{V}+f\boldsymbol{k}\times\boldsymbol{V}$$
$$=-g\,\nabla z+\nu\,\nabla^2\boldsymbol{V}, \tag{1a}$$
$$\left(\frac{\partial}{\partial t}+(\boldsymbol{V}\cdot\nabla)\right)(z-h)+(H+z-h)\nabla\cdot\boldsymbol{V}$$
$$=\kappa\,\nabla^2 z+\boldsymbol{F}, \tag{1b}$$

where $\boldsymbol{V}$ is the horizontal velocity, $z(\boldsymbol{r})$ is the perturbation of the free surface with respect to its mean hight H, g is the acceleration of gravity, $h(\boldsymbol{r})$ is the height of the topography, ν and κ are the dynamical and thermal diffusion coefficients, and $\boldsymbol{F}$ is the forcing. The velocity is then written as the sum of divergent and rotational components which transform the equations to ones in the velocity potential, χ, and the streamfunction, Ψ. The equations are then written in terms of their Laplacians, the divergence and the vorticity. Each equation (divergence, vorticity, and height equations) is then expanded in terms of three cosine basis functions with the wave numbers forming a triad. The system reduces to a set of nine ordinary differential equations for x_i, y_i, and z_i which are the coefficients of the potential, streamfunction, and height fields respectively. The indices vary cyclically as $(i, j, k)=(1,2,3)$, $(2,3,1)$, or $(3,1,2)$. The resulting truncated PE model is:

$$a_i\dot{x}_i=a_ib_ix_jx_k-c(a_i-a_k)\,x_jy_k$$
$$+c(a_i-a_j)\,y_jx_k-2c^2y_jy_k$$
$$-\nu_0a_i^2x_i+a_i(y_i-z_i), \tag{2a}$$
$$a_i\dot{y}_i=-a_kb_kx_jy_k-a_jb_jy_jx_k$$
$$+c(a_k-a_j)\,y_jy_k-a_ix_i-\nu_0a_i^2\,y_i, \tag{2b}$$
$$\dot{z}_i=-b_kx_j(z_k-h_k)-b_j(z_j-h_j)\,x_k$$
$$+cy_j(z_k-h_k)-c(z_j-h_j)\,y_k$$
$$+g_0a_ix_i-\kappa_0a_iz_i+F_i, \tag{2c}$$

where a_i, b_i, and c are combinations of the wavenumbers and ν_0 and κ_0 are nondimensional diffusion coefficients. Additional parameters of the problem are g_0, the nondimensional gravitational constant; h_i, the topography; and F_i, the components of the mass source/sink forcing. For a more detailed derivation see Lorenz (1980).

We use parameter values in keeping with previous studies (Lorenz, 1980; Gent and McWilliams, 1982; Vautard and Legras, 1986; Lorenz, 1986; Warn and Menard, 1986; Curry and Winsand, 1986), specifically $a_1=a_2=1$, $a_3=3$, $c^2=3/4$, $g_0=8$, $\nu_0=\kappa_0=1/48$, $h_1=-1$, $h_2=h_3=0$, and $F_2=F_3=0$. The forcing is incorporated in F_1, a free parameter. We study the effectiveness of several initialization methods for low ($F_1\leqslant 0.1$) to moderate ($0.1<F_1\leqslant 0.4$) values of this parameter.

For our purposes, we regard the truncated PE (2) as the full model. The most basic approximation to this system is a quasi-geostrophic (QG) model. This simplified model is equivalent to the lowest order expansion in Rossby number and is written as

$$\text{QG}: (a_ig_0+1)\,\dot{z}_i=F_i+g_0c(a_k-a_j)\,z_jz_k$$
$$-a_i\nu_0(a_ig_0+1)\,z_i+c(h_jz_k-h_kz_j), \tag{3}$$

with $y_i=z_i$ and $a_ix_i=c(a_k-a_j)\,z_jz_k-a_i(\dot{z}_i+\nu_0a_iz_i)$. If forcing, damping, and topography are ignored, (3) is the *minimum equation* triad system studied by Lorenz (1960) and has Jacobi elliptic functions as solutions. The system (3) is easy to work with and does not admit gravity waves; however, its solutions do qualitatively represent the solutions of the PE system in a narrow parameter regime, as noted by Lorenz (1980), Gent and McWilliams (1982), and Curry and Winsand (1986).

There are a variety of model systems intermediate to the PE and QG. The intermediate models have been derived by Gent and McWilliams (1982) who then compared them for various values of forcing. This work was carried further by Curry and Winsand (1986). A somewhat more realistic approximation to the PE model is the intermediate model called balanced equations (BE). Just as with QG, this approximation also excludes gravity waves. In the BE the potential, vorticity and streamfunction equations, (2a) and (2b), are the same as for the PE while equation (2c) is replaced by the balance condition:

$$\text{BE}:\quad a_iy_i-2c^2y_jy_k=a_iz_i. \tag{4}$$

Thus, the number of degrees of freedom is intrinsically reduced to three, the Rossby modes. Equation (4) is the same condition used by Lorenz (1980). He showed that the attractor for (4) appeared graphically the same as that for (2). Gent and McWilliams (1982) conclude that "the solutions of BE are virtually indistinguishable from the superbalance equation." Curry and Winsand (1986) concur after an exhaustive study of the bifurcations of the various intermediate models. Vallis (1992) demonstrates that the balance condition is an effective initialization, but that it cannot eliminate all gravity wave activity in a PE integration. Sundermeyer and Vallis (1993) demonstrate similar correlation dimension for the PE and BE when $F_1 < 0.24$. After that, the correlation dimension of the PE is greater than 3.

The main point here is that the BE bifurcation sequence closely parallels that of the PE, the transition values occurring at nearly the same values of forcing as in the PE model. The other intermediate models qualitatively show the same series of bifurcations but the numerical values of the forcing at which they occur differ significantly.

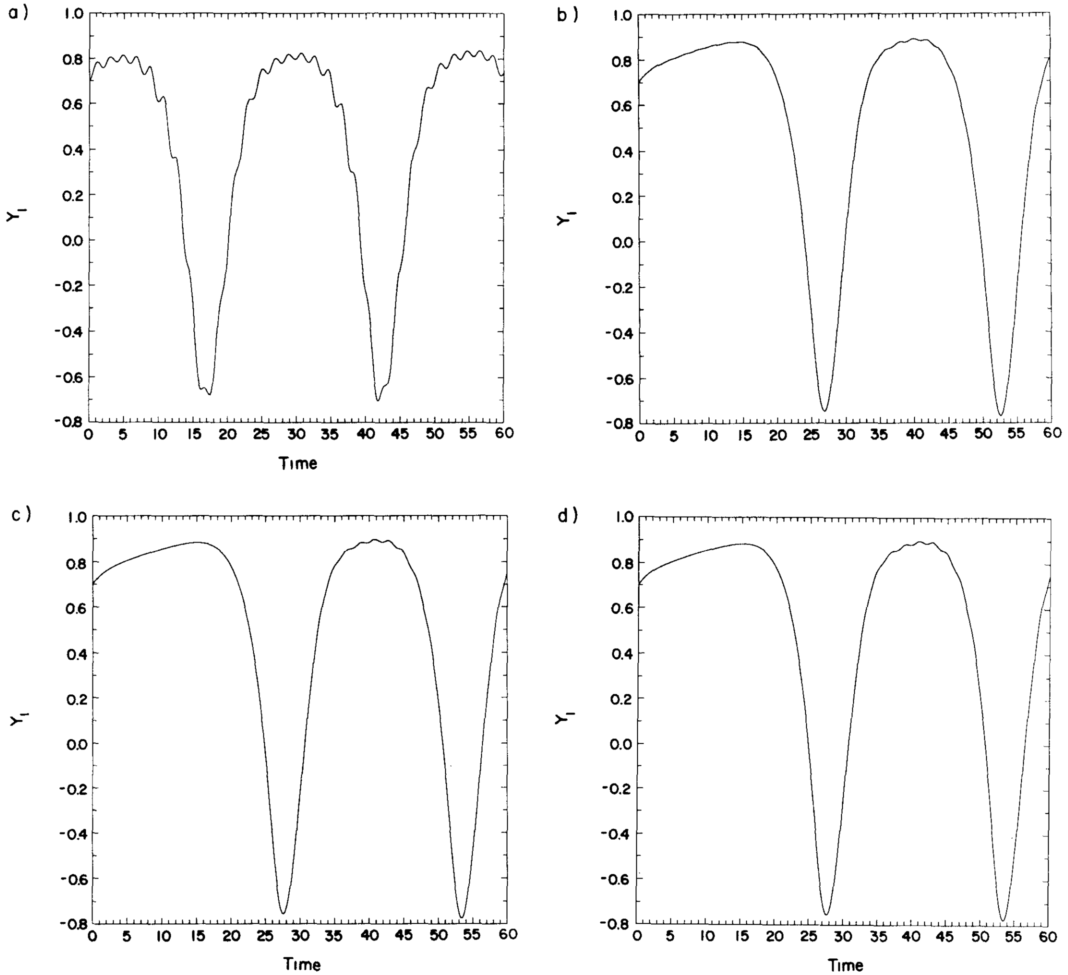

Fig. 1. Behavior of y_1 in time to $t = 60$ for $F_1 = 0.245$ for differing initializations. (a) PE initialized at t_{500}, (b) PE with Lorenz initialization, one derivative zeroed, (c) PE with Lorenz initialization, 3 derivatives zeroed, (d) PE with Lorenz initialization, 20 derivatives zeroed, (e) PE initialized with minimization, 3 derivatives, (f) PE initialized with minimization, 20 derivatives, (g) PE initialized with balanced condition, and (h) BE initialized with balanced condition.

3. Initialization

The goal of initialization algorithms is to determine a balanced state of the atmosphere. This goal is equivalent to establishing a functional relationship between one set of phase space variables and another set of phase space variables. If such a functional relationship exists then it defines a manifold.

For low-order systems, several initialization methods have been proposed which are systematically investigated in this section. Lorenz (1980) noted that when the 9 equation PE was integrated in time and the forcing parameter was sufficiently small, the high frequency oscillations attributed to gravity wave activity eventually died out and the resulting motion on the attractor was "nearly" quasigeostrophic. The quasigeostrophic attractor, Lorenz concluded, was 3-dimensional and therefore 3 variables defined the other 6 variables in the 9-dimensional phase space. That is, 6 variables, presumably the gravity modes, were functionally related to the three dimensional quasigeostrophic attractor was globally attracting, invariant, and contained the gravity wave-free submanifold, the *slow manifold*. Following Lorenz (1980), we let the

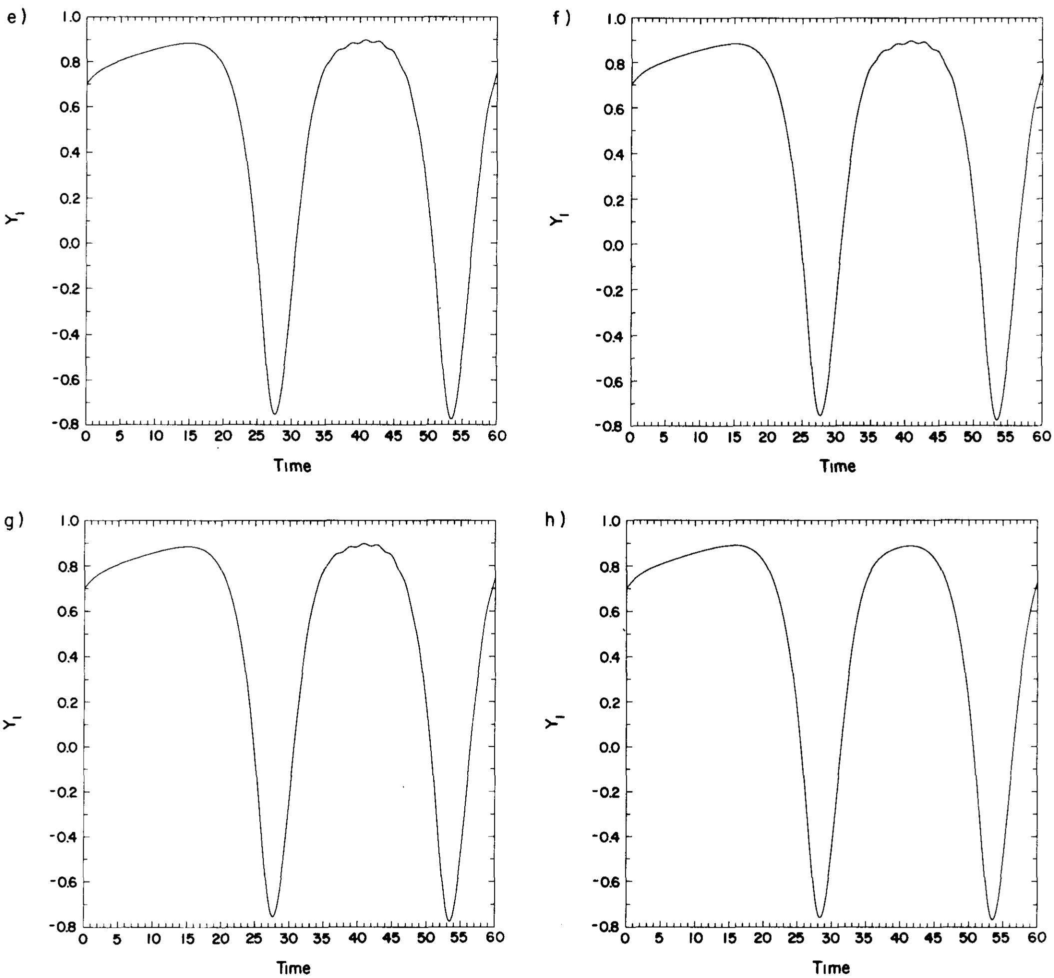

Fig. 1 (cont'd).

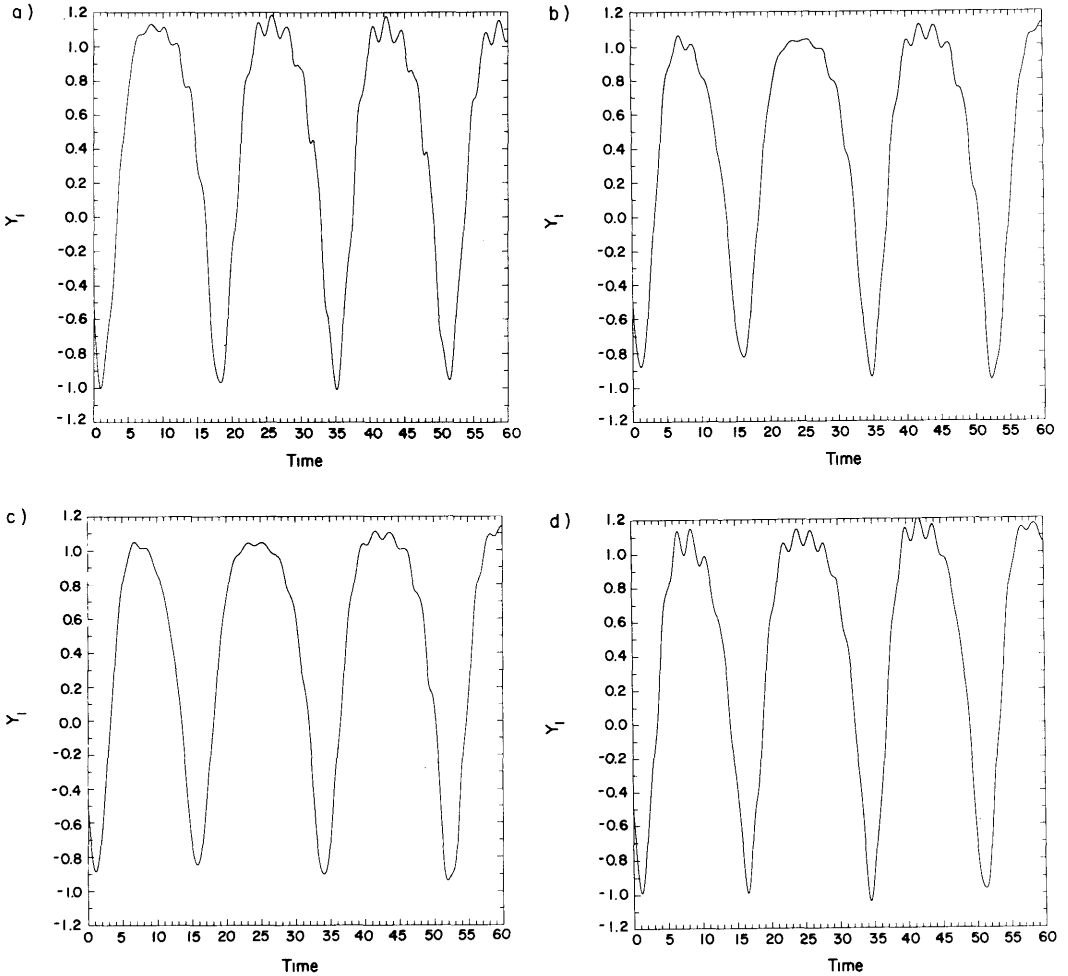

Fig. 2. As for Fig. 1 with $F_1 = 0.4$.

y equations of the PE (2b) represent the Rossby modes and the remaining 6 equations, (2a) and (2c), the gravity modes.

Most previous studies have explored initialization of (2) for relatively modest values of F_1 ($\leqslant 0.1$). In this section, we choose instead to investigate somewhat larger values of the forcing where it may be more difficult to remove gravity waves through an initialization process. Curry and Winsand (1986) showed that for $F_1 = 0.24$, a new strange attractor appears. (See also Vautard and Legras, 1986 and Sundermeyer and Vallis, 1993.) The following examples are for forcings of $F_1 = 0.245$ and $F_1 = 0.4$ (Figs. 1 and 2, respectively) which is in the regime of the new strange attractor. We are motivated by the question of how initialization algorithms perform in the presence of self sustained gravity wave activity.

Since gravity waves quickly decay for modest values of the forcing, the simplest approach to decreasing the gravity wave activity is numerical time integration of the equations of motion of a large number of time steps to allow this natural decay. This approach is used here as a base case to compare with the other methods. The PE is integrated for 500 time units, that is to t_{500} and the state at that time is used as the initial condition for all subsequent time integrations and as the begin-

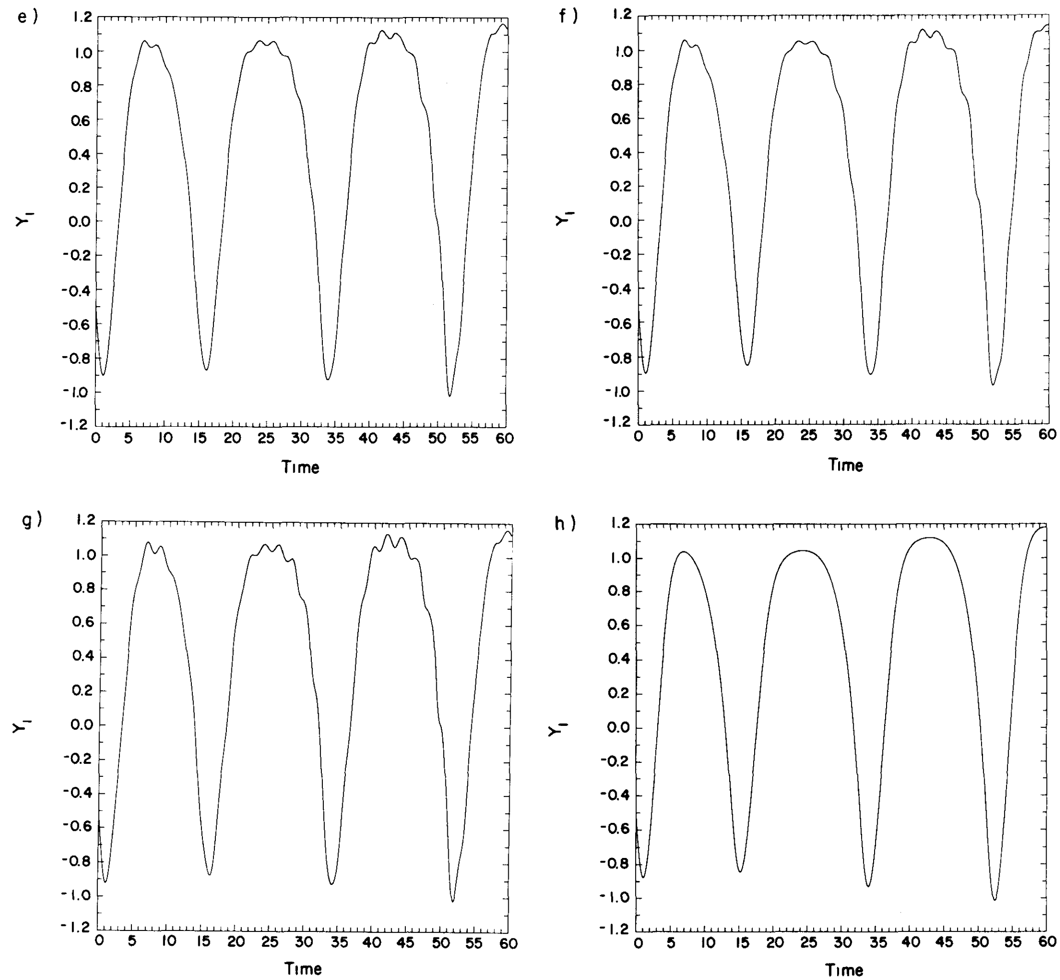

Fig. 2 (cont'd).

ning state for the subsequent initialization studies. Both the PE (2) and BE (4) are integrated using the standard fourth order Runge-Kutta method.

Fig. 1a ($F_1 = 0.245$) and 2a ($F_1 = 0.4$) illustrate the evolution of y_1, a streamfunction component in the PE using an initial condition of the state at t_{500}. In both cases, high frequency oscillations (gravity waves) are clearly evident throughout*. Hence, in this parameter regime, gravity wave activity does persist.

3.1. *The Lorenz method*

The second method investigated, due to Lorenz (1980), expands on the idea that a good initialization strategy should begin by setting the time tendency of the gravity modes to zero. In this strategy it is assumed that the frequency of the gravity waves is an order of magnitude larger than that of the Rossby modes (by a factor of k) and that any phase point is resolvable into Rossby and gravity components. If such a representation is possible, the nth time derivative of the gravity modes should be larger by a factor of k^n than the

* Although only y_1 is plotted here, the other variables behave similarly. We choose to show the full behavior of y_1 here rather than to subtract off some mean state. The behavior of an anomaly field tends to be dominated by differences in phase that hide the effects of the gravity waves.

corresponding Rossby modes. The algorithm proceeds iteratively and sequentially by setting the nth time derivative of the gravity mode components of an arbitrary intial condition to zero until $n = N$, some arbitrary but large number. The gravity wave tendencies should then be effectively eliminated to the Nth order.

To implement the method, following Lorenz (1980), we separate the components of the system into the Rossby modes, $\boldsymbol{Y} = (y_1, y_2, y_3)^{\mathrm{T}}$, and the gravity modes, $\boldsymbol{X} = (X_1, X_2, ..., X_6)^{\mathrm{T}} = (x_1, x_2, x_3, z_1 - y_1, z_2 - y_2, z_3 - y_3)^{\mathrm{T}}$. The superscript $^{\mathrm{T}}$ denotes the vector transpose. In this method, referred to here as *successive zeroing*, the time derivatives of the gravity modes are set to zero by solving $\mathrm{d}^n\boldsymbol{X}/\mathrm{d}t^n = 0$ ($n = 1, 2, ..., N$) using Newton's method,

$$\boldsymbol{X}^{l+1} = \boldsymbol{X}^l - \left[\frac{\partial(\mathrm{d}^n\boldsymbol{X}^l/\mathrm{d}t^n)}{\partial \boldsymbol{X}^l}\right]^{-1}\left(\frac{\mathrm{d}^n\boldsymbol{X}^l}{\mathrm{d}t^n}\right), \tag{5}$$

where the superscripts, l represent the iteration index. The Jacobian matrix of derivatives is computed using a finite difference approximation for each component. Convergence is assumed when $\|\boldsymbol{X}^{l+1} - \boldsymbol{X}^l\| < \delta$, for δ sufficiently small. When the iteration has converged for the nth derivative, we continue to zero the $(n+1)$th, and so forth to some $n = N$.

A few details should be noted about this method. First, since the zeroing is successive, zeroing the $(n+1)$st derivative does not guarantee that the nth derivative or any other lower order derivatives remain zero. Second, when the order of the derivative becomes large ($N \sim 35$), the convergence criteria no longer guarantees that the computed derivatives are small. "Convergence" is still obtained; but, for example, when $\delta = 10^{-20}$, the norm of the 50th derivative of the Jacobian matrix was $\mathrm{O}(10^5)$. This phenomena can be traced to the fact that the Jacobian matrix is nearly singular for large N. This is analogous to the behavior of the so called unnormalized power method for computing eigenvalues in numerical analysis (Stoer and Bulirsch, 1980). For many such numerical problems, increasing the number of degrees of freedom necessarily precludes some norm of a large matrix from being small.

For $F_1 = 0.245$, the results of Lorenz initialization are shown in Figs. 1b, c, and d for zeroing the first 1, 3, and 20 derivatives respectively. In each case, we begin our study with the phase space point generated at t_{500}, then successively zero the derivatives. Lorenz (1980) demonstrated that zeroing the first three derivatives is sufficient to get close to the slow manifold for modest forcing (approximately $F_1 \leqslant 0.1$). This study reinforces that conclusion for larger values of the forcing. Illustration 1b has a much smoother appearance than does figure 1a due to the suppression of high frequency waves by this initialization strategy. However, gravity waves are evident on the second peak and possibly even visible on the first peak of this figure. Zeroing three derivatives (panel 1c) effectively removes the gravity wave tendency from the first peak but not the second. Zeroing 20 derivatives (panel 1d) gives no additional improvement. The same general pattern is evident in figures 2b, c, and d when $F_1 = 0.4$. Twenty zeroed derivatives (panel 2d), in fact, shows more gravity wave activity than for three zeroed derivatives (panel 2c). This is due to the fact that the zeroing occurs successively. After many derivatives are successively zeroed, there is no reason to expect that the lower order derivatives should still be small. And indeed, we find that they are not. This finding is very parameter dependent.

3.2. *Minimization*

To circumvent the problem of reappearance of the low order derivatives, we modify Lorenz's algorithm so that the zeroing of the N derivatives occurs simultaneously. The resulting "minimization" problem is then to make all the derivatives as close to zero as possible. We minimize the Euclidean norm of the $6N$-dimensional system, i.e.,

$$\left\|\frac{\mathrm{d}\boldsymbol{X}}{\mathrm{d}t}\right\| = \left(\left(\frac{\partial X_1}{\partial t}\right)^2 + \cdots + \left(\frac{\partial X_6}{\partial t}\right)^2 + \left(\frac{\partial^2 X_1}{\partial t^2}\right)^2 + \cdots + \left(\frac{\partial^2 X_6}{\partial t^2}\right)^2 + \cdots + \left(\frac{\partial^N X_1}{\partial t^N}\right)^2 + \cdots + \left(\frac{\partial^N X_6}{\partial t^N}\right)^2\right)^{1/2}. \tag{6}$$

Figs. 1e, f show the results of minimizing 3 and 20 derivatives respectively for $F_1 = 0.245$. For this forcing, no noticeable change has occurred from successive zeroing. For the larger forcing value of 0.4 in Fig. 2e, we see that minimization does not significantly reduce the gravity wave activity when compared to successive zeroing of three derivatives; however, when the tendency of the first 20 zero derivatives are examined (Fig. 2f), the minimization clearly smooths the gravity waves better than successive zeroing. When comparing panel 2f with 2d, it is clear that the lower order derivatives do reappear when zeroing is carried out successively. Hence, this algorithm has its greatest effect for those values of the forcing where there is intense gravity wave activity and when the smoothest evolution possible is desired. Indeed, for high forcing values a possible strategy would be to determine a minimum, then evolve for one time step and repeat the minimization time step. This approach would be computationally expensive.

3.3. *Balance equation*

The final method investigated is to "apply" the BE itself as an initialization method. Specifically,

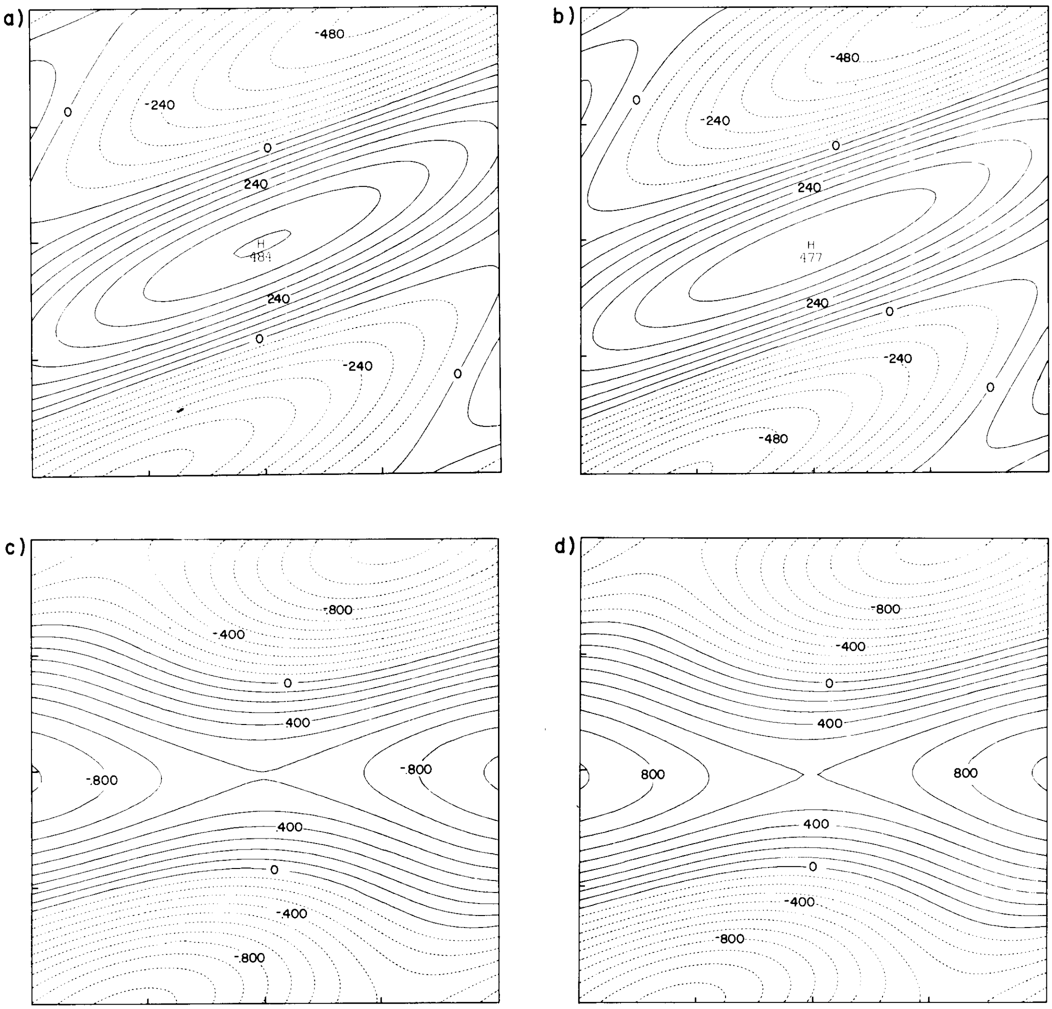

Fig. 3. Comparison of divergence and height fields for the Lorenz method and for application of the balanced condition for $F_1 = 0.25$. The scales of the figures are 2π periodic in x and y. (a) Divergence field for Lorenz's method, 4 derivatives zeroed, (b) divergence field for balanced condition, (c) height field for Lorenz's method, 4 derivatives zeroed, and (d) height field for balanced condition.

for given y_i, the z_i are computed from (4). An implicit equation for the x_i is found by taking the time derivative of (4) and substituting the derivatives of y_i and z_i from (2b) and (2c) (Gent and McWilliams, 1982).

This balanced condition applied to the phase space point determined at t_{500} (Figs. 1g, 2g) is roughly equivalent to zeroing three derivatives, but costs significantly less. Integration using the BE model is included in panels 1h and 2h for comparison. Clearly, the qualitative behavior of the BE is similar to the PE model but without gravity wave activity.

3.4. Comparison of methods

Although it is reasonably easy to find initialization strategies which reduce the time tendency of gravity wave activity for modest values of the forcing, the examples cited above demonstrate that it is not so easy to initialize models when the forcing is larger and self sustaining gravity activity is present.

Successive zeroing of three derivatives produces

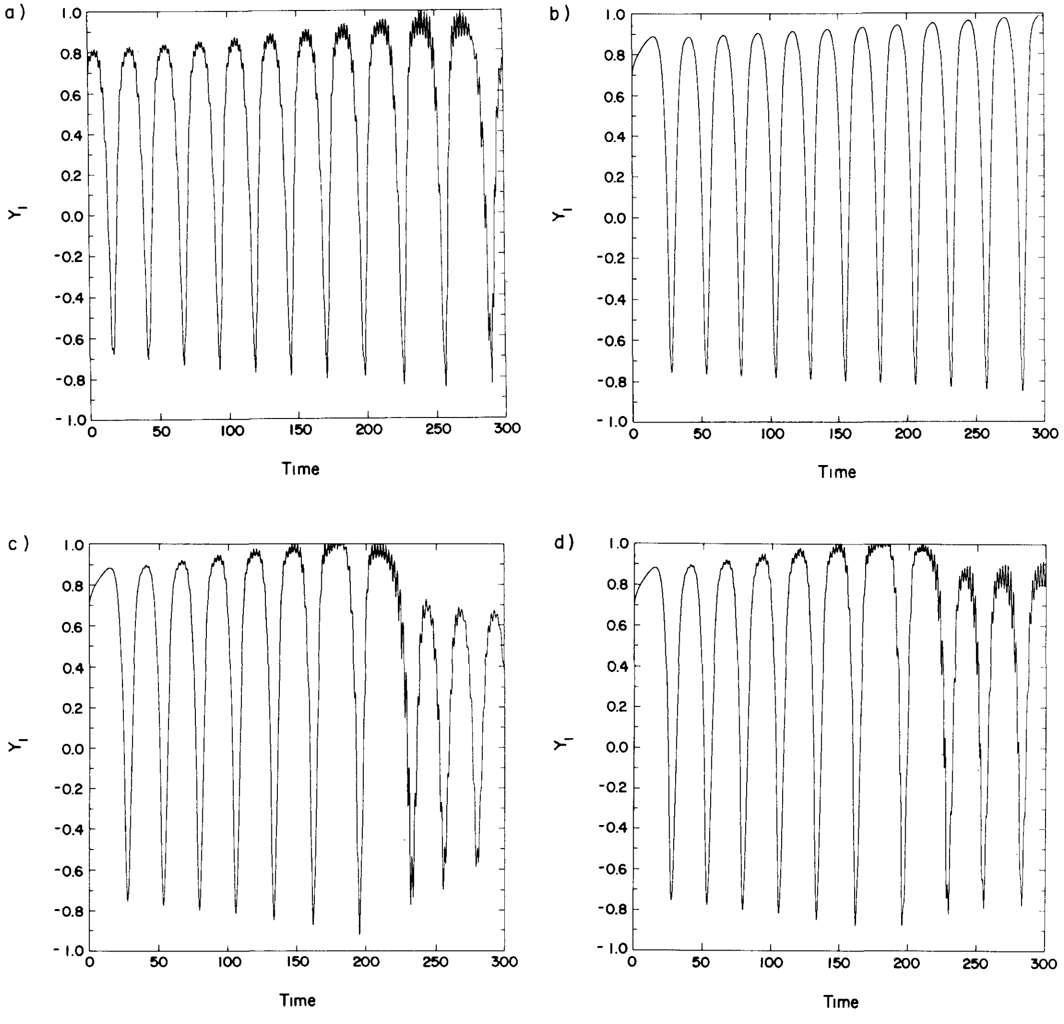

Fig. 4. Behavior of y_1 to $t = 300$ for $F_1 = 0.245$ for initializations (a) PE initialized at t_{500}, (b) BE initialized with balanced condition, (c) PE with Lorenz initialization, 3 derivatives zeroed, and (d) PE initialized with balanced condition.

as smooth a solution, to the eye, as any other method. Successively eliminating the tendency of a large number of gravity wave derivatives (20 here) did not produce a smoother trajectory than when a few (3) derivatives were zeroed for these moderate values of F_1. This strategy demonstrates, however, that for higher values of the forcing the time tendency of the lower order derivatives become nonzero when many derivatives are successively zeroed. We mitigate this problem by introducing a strategy which simultaneously minimizes the norm of the sum of the squares of all derivatives. An advantage of this method is that very high quality minimization software can be used and this effectively reduces the practical initialization problem to a much studied one.

Application of the balanced condition produced results similar to zeroing the first several time derivatives. Fig. 3 shows the divergence and height fields for the Lorenz method with four derivatives zeroed as well as the consequence of applying the balance condition for a forcing of $F_1 = 0.25$. The similarity of the plots for these two different initialization strategies suggest that they are representations of similar solutions. At lower forcing ($F_1 = 0.1$, not shown here) the fields are indistinguishable. Fig. 4 compares successive zeroing and BE initialization more closely for a longer time integration (to $t = 300$ units) for $F_1 = 0.245$. Panel 4a is the time integration using the PE with the same t_{500} point used in Fig. 1. The BE integration is shown in 4b for comparison. Illustrations 4c, d start with phase points which have been initialized by zeroing three derivatives successively and from satisfying the balance condition respectively. Both Figs. 4c, d show an initial absence of oscillatory behavior; but oscillations do develop in time. Note that at about time $t = 210$ the gravity wave activity is less for the BE initialized run than for that initialized with three zeroed derivatives. Further, Fig. 4c shows that the amplitude of the rotational modes as well as the superimposed gravity modes decays for longer times when three derivatives are zeroed. This does not occur in either the uninitialized PE run or in the BE run. Similar behavior is observed at other points. We infer that the run initialized using the balanced condition remains closer to a manifold with reduced gravity wave activity and is likely to provide the better initialization method, at least for the parameter regime studied.

4. The slow manifold of order N

The strategies for initializing the nine equation system (2) investigated in the previous section all show some success in determining initial conditions leading to subsequent damping of gravity waves. However, none were successful in totally eliminating these high frequency waves for larger values of the forcing. Possible explanations include (1) that a slow manifold does not exist in this parameter range, or (2) that the methods used and the best precision available is inadequate in finding phase space points on the desired manifold.

Here we study the Lorenz model for lower values of the forcing. We will review and expand on studies of the bifurcations of the model and then directly address the issue of using Lorenz's method to compute points on the desired manifold.

4.1. Model bifurcations and gravity waves

The BE, as well as the PE and other intermediate models undergo a series of bifurcations as a function of the forcing. These bifurcations have been defined in relation to dynamics about the Hadley fixed point (zonal flow) (Gent and McWilliams, 1982; Curry and Winsand, 1986; Vautard and Legras, 1986) defined by

$$x_1 = v_0 a_1 y_1, \tag{7a}$$

$$y_1 = \frac{F_1}{a_1 v_0 (1 + a_1 g_0 + v_0^2 a_1^2)}, \tag{7b}$$

$$z_1 = (1 + v_0^2 a_1^2) y_1, \tag{7c}$$

$$x_2 = x_3 = y_2 = y_3 = z_2 = z_3 = 0. \tag{7d}$$

In the PE, the Hadley solution is stable for $F_1 < 0.01493$ at which point there is a pitchfork bifurcation. This produces a pair of stable fixed points. However, the resulting one-dimensional unstable manifolds which are associated with this pitchfork transition for the Hadley fixed point become part of the boundary of what will become the strange attractor (Curry and Winsand, 1986). The Hadley solution bifurcates further via a Hopf bifurcation at $F_1 = 0.0774$ (Krishnamurthy, 1985) and produces an unstable periodic orbit. Then, more globally, ensues a range of interleavings between strange attractors and period doubling bifurcations. However, after the Hopf bifurcation

(Krishnamurthy, 1985), the unstable manifold of the Hadley solution has increased in dimension from one to three. This three-dimensional manifold also becomes part of the boundary of the strange attractor.

More concretely, the first column of Table 1 lists the eigenvalues of the Jacobian matrix evaluated at the Hadley fixed point for $F_1 = 0.07$. The fixed point is unstable as implied by the real part of at least one eigenvalue being positive. Additionally, there are three pairs of complex conjugate eigenvalues with negative real parts leading to a damped oscillation (equivalent to a contracting trajectory in its eigenspace). These are the gravity waves. The remaining eigenvalues are real (Rossby waves) with two contracting directions (negative values) and one unstable expanding (positive) direction. The second column is for $F_1 = 0.08$. We see that there has been a further bifurcation as one of the complex conjugate pairs of eigenvalues has crossed into the right half of the complex plane; there are now three unstable dimensions. By the Hartman–Grobman Theorem (see Guckenheimer and Holmes, 1983), if there is a three dimensional manifold containing gravity wave oscillations in the linearized system it also exists in the nonlinear system. Therefore, we do not expect sustained gravity wave oscillations for $F_1 \leqslant 0.07$, but for values of $F_1 \geqslant 0.08$ gravity waves must be present in the global attractor. This, however, does not rule out the possibility that there could be a submanifold which is slow.

Table 1. *Eigenvalues of the Jacobian matrix computed at the Hadley point*

$F_1 = 0.07$		$F_1 = 0.08$	
real	imaginary	real	imaginary
−0.0208	3.0000	−0.0208	3.0000
−0.0208	−3.0000	−0.0208	−3.0000
−0.0678	5.0536	−0.0693	5.0650
−0.0678	−5.0536	−0.0693	−5.0650
−0.0034	2.9635	0.0012	2.9604
−0.0034	−2.9635	0.0012	−2.9604
0.0967	0.0000	0.1088	0.0000
−0.2041	0.0000	−0.2226	0.0000
−0.0208	0.0000	−0.0208	0.0000

4.2. *Slow manifold points of order N*

Here we will use the proof strategy of the Newton-Kantorovich Theorem together with the Nested Interval Property to find points corresponding to a gravity wave-free (to order N) locally invariant manifold, at least for lower values of the forcing.

As we have already seen (Subsection 3.1, Lorenz's method), Newton's method (formally known as the Newton-Kantorovich method) is a very powerful tool for solving nonlinear equations. Further, if the hypotheses of the Newton-Kantorovich Theorem are satisfied, then it guarantees that a unique solution to the nonlinear equation not only exists, but that the Newton iteration sequence starting from a "good" initial condition must converge to that solution. As noted in Subsection 3.1, if the components of the nine variable equations of motion are resolved into gravity waves and Rossby waves, then the nth derivative of the gravity wave portion of the motion must exceed that of the Rossby portion by a factor of k^n.

Our strategy for finding a point on the desired manifold requires two stages. First the Lorenz initialization strategy is applied, successively solving $\mathrm{d}\boldsymbol{X}/\mathrm{d}t = 0$, $\mathrm{d}^2\boldsymbol{X}/\mathrm{d}t^2 = 0, \ldots$. Solving $\mathrm{d}^n\boldsymbol{X}/\mathrm{d}t^n = 0$ produces $\boldsymbol{X}_n$, a state for which the Newton-Kantorovich iteration has sufficiently converged. This most recent state, $\boldsymbol{X}_n$, is the initial condition for the iteration to solve $\mathrm{d}^{n+1}\boldsymbol{X}_n/\mathrm{d}t^{n+1} = 0$. (This procedure is applied here to several points in the low forcing ($F_1 \leqslant 0.1$) parameter range.) Such points are not particularly near to the Hadley fixed point. The second step in our approach is to use the Newton-Kantorovich Theorem to determine the radii of a nested sequence of closed and bounded sets whose intersection must asymptotically contain only one point. That point would lie on the desired slow manifold. The conditions, details, and application of the theorem are presented in Appendix A. If steps one and two are realized then we have achieved our goal of finding "slow points."

The radius (r_0) of the ball containing the solution of (5) is computed for each order of the derivative and is plotted in Fig. 5 ($F_1 = 0.07$). Each of the balls computed is embedded in the ball of the previous derivative, forming a nested sequence of sets. The size of the ball containing the exact solution decreases geometrically as more derivatives are zeroed. This evidence suggests that there exists a sequence of nested compact balls of geometrically decreasing size, each containing a unique

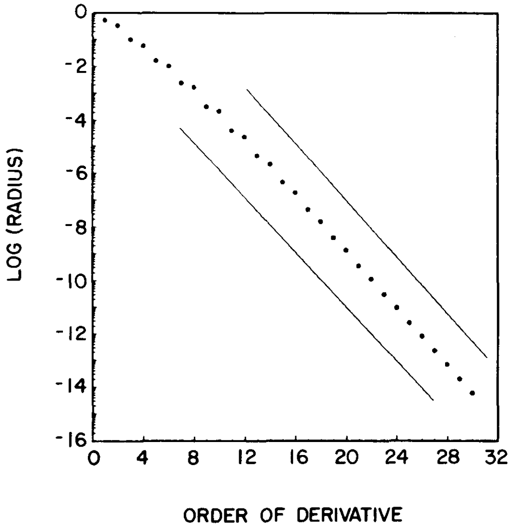

Fig. 5. The computed logarithm of the size r_0 of the Newton-Kantorovich sphere as a function of the order of the derivative zeroed for $F_1 = 0.07$. The balls are nested and the decrease in r_0 is exponential with n. The lines bound the slope between -0.51 and -0.53.

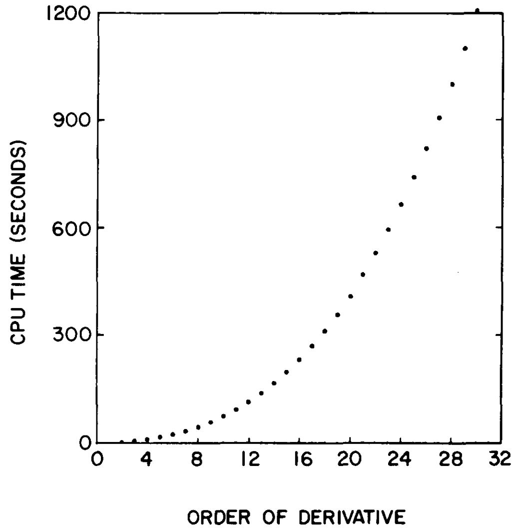

Fig. 6. The CPU time required to compute r_0 in Fig. 5 as a function of the order of the derivative zeroed.

solution of zeroing the nth derivative. By the "Nested Interval Property", if the result were not asymptotic we could conclude that there exists a unique point that is the intersection of these sets*.

The exponential decrease in radius suggests that if one could zero an infinity of derivatives, one could conclude that there exists a limit point which is in the intersection of all these sets and this limit point would be free of gravity wave activity (as defined by the Lorenz method of zeroing time derivatives) and hence a slow point would have been determined. Fig. 6 plots the CPU time required to zero each derivative presented in Fig. 5. Since the increase in CPU time is clearly exponential, it is impossible to exactly determine a slow point in this manner. However, the power of the Newton-Kantorovich Theorem and the exponentially decreasing size of the nested balls is strong evidence that a point exists. We obtained similar results for two other points at this forcing ($F_1 = 0.07$) as well as for three points for $F_1 = 0.1$. Hence, for at least these low forcing values we could conclude that slow points exist in the presence of infinite precision and a persistence of the asymptotic rate of decrease in the radii of the enclosing balls. Because the hypotheses of the Newton-Kantorovich theorem have been checked, one could conclude that the points of order N lie on a manifold of order N.

When the Newton-Kantorovich computation was performed for $F_1 = 0.245$, we again noticed a decrease in the size of the balls containing the solution; however, in this case, the balls were not always nested. A consequence is that slow points of order M are not always close to slow points of order N. Since the Nested Interval Property no longer holds, we are no longer able to conclude that the slow manifold exists for this higher value of the forcing. This does not mean that the manifold does not exist. It merely means that the realm of validity of our strategy does not reach to this higher value of the forcing.

Finally, note that when the logarithm of the

* In particular, Bartle and Sherbert (1982) states that for a nested sequence of closed bounded nonempty intervals, $I_n = [a_n, b_n]$, $n \in N$, there exists a number $\xi \in \mathfrak{R}$ so that $\xi \in I_n$ for all $n \in N$. In addition, if the lengths, $b_n - a_n$, of the intervals converge to zero, then the common element ξ is unique. The one-dimensional theorem is readily generalizable to our multi-dimensional context. As applied to the calculation of points on the slow manifold, the exponential decrease of the size of the balls implies that a unique "slow" point will exist if the balls are nested.

sequence of radii decreases linearly then the radii themselves decrease exponentially. The slope of the bounding lines in Fig. 5 is roughly $-\frac{1}{2}$. This is for low values of the forcing. Therefore, the radii decrease as

$$\log r_n = -\tfrac{1}{2}n + b, \tag{8}$$

so that

$$r_n = C10^{-n/2}, \tag{9}$$

where b and C are constants such that $C = e^b$. Eq. (9) implies that we would need to zero 20 derivatives to obtain 10 digits of accuracy. In practice, we obtain this accuracy with fewer derivatives zeroed. This result confirms Lorenz's observations that zeroing out a few derivatives would provide a good approximation to a point on the slow manifold. We believe that this asymptotic result has significant potential utility.

5. Conclusions

We have examined various strategies for initializing the 9-equation system of Lorenz. For moderate values of the forcing, we have established a hierarchy of initialization methods which approximate to order N intial conditions on the slow manifold. We find that not only as noted in previous articles do the bifurcation sequences of BE closely mimic that of PE but also the Balance Equation model comes closest to projecting onto the slow manifold of the PE. Further, solving the BE is easier and requires far less computer time than competing methods. This strongly recommends the BE for further study in initializing more realistic systems (Spall and McWilliams, 1991).

When applying the original Lorenz initialization method for values of the forcing less than or equal to 0.1, three derivatives are usually sufficient to determine a good approximation to a gravity wave-free state. This is explained by the analysis in the previous section, which indicates an exponential rate of convergence to slow points when the model is experiencing low forcing. The surprising feature of Lorenz's method is that while our analysis indicates that ten derivatives would be necessary to achieve a 20-digit accuracy for a slow state, in actual applications three is often adequate. For moderate values of the forcing (0.245 and 0.4) each algorithm could successfully zero several derivatives but both higher and lower order derivatives eventually become nonzero, *in sharp contrast* to the behavior observed for forcing values around $F_1 = 0.1$. One possible interpretation of the return of the gravity wave oscillations for higher values of the forcing is that the algorithm for finding slow points fails to converge for this range of parameters. Another is that the slow manifold no longer exists in this parameter range. As indicated in Section 4, we believe that standard initialization strategies must fail due to the finiteness of machine precision and the computation time. However, since the correlation dimension of the PE exceeds three for $F_1 > 0.24$ (Sundermeyer and Vallis, 1993), there is a possibility that the slow manifold ceases to exist at that parameter value or else may simply become unstable.

We have also introduced a strategy which simultaneously minimizes derivatives. This method has the advantage of using software which is widely available. However, for moderate values of the forcing ($F_1 = 0.245$ or 0.4) this strategy does not produce significantly different states of the system than produced by successively zeroing only three derivatives. For 20 zeroed derivatives, the minimization strategy does produce solution curves having less gravity wave activity than for successive zeroing of the 20 derivatives (Fig. 2f is smoother than 2d). For these larger values of the forcing, every solution of the PE initial value problem displays some high frequency oscillations. It should be noted that the strategy for determining slow points in Section 4 could be suitably modified to determine a "slowest point" which would also lie on a manifold. The approach would be to use standard minimization software and the ideas from Section 4.

The final method studied here uses the initial data from a low-order balance equation model to initialize the primitive equations. This approach has the best success of all methods we have tried. This leads to the speculation that the attractor of the BE is close to that of the PE. It further suggests that the BE must be seriously considered in any further analyses of initialization strategies.

Finally, we have determined several points on the locally invariant slow manifold of order N (forcing 0.07 and 0.1) by applying the *Newton-Kantorovich Theorem* and demonstrating that there exists a solution for each succeeding order of derivative zeroed and that such solutions lie in concentric spheres of exponentially decreasing radii. Then by appealing to the *Nested Interval Property*, we conclude that slow points exist in the presence of infinite precision; that is, there would be phase points in the PE model which are devoid of gravity wave activity. We conclude that there exists a locally invariant three dimensional manifold for which the higher frequency gravity oscillations are determined by the Rossby modes, at least for lower values of the forcing. This manifold is contained in the attractor. The attractor is composed of many submanifolds, including sets defining manifolds of order N, and countably many of which contain gravity waves (Section 3) and at least one which is locally invariant, slow, and attracting (Section 4). By "slow", we mean that the time tendencies of the gravity waves are zero, that is, that Lorenz's method would converge for both an infinite number of derivatives and an infinite amount of precision. We have also shown that it is impractical to compute such points exactly by this method since CPU time increases exponentially with the degree of derivative zeroed.

Warn and Menard (1986) report that they found a submanifold that contains gravity waves

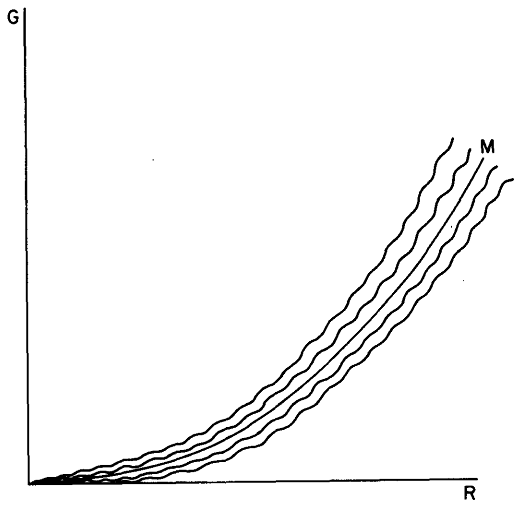

Fig. 7. Schematic of Slow manifold. The R-axis denotes the rotational manifold and the G-axis the gravitational manifold. The curve labeled M denotes the slow manifold. Wavy lines are nearby manifolds containing gravity waves.

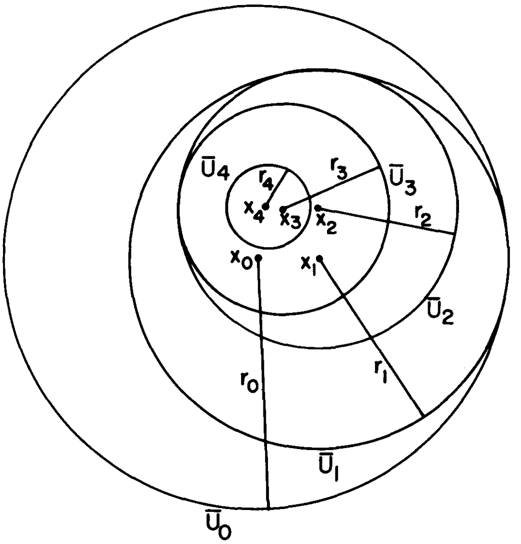

Fig. 8. Schematic of nested balls of Newton-Kantorovich iteration projected onto a 2-dimensional plane.

for the same values of the forcing studied here. Errico (1982, 1984) came to the same conclusion for different systems. We maintain that this does not necessarily imply that the slow manifold is either "fuzzy" or does not exist, but rather that there are likely to be gravity wave-containing manifolds "close" to any phase point on the attractor and the resolution only comes with infinite precision. (Our vision of the slow manifold is depicted schematically in Fig. 7). The axes are the Rossby and gravity manifolds respectively. The smooth curve labeled M is the slow manifold. Close to the slow manifold are many "wavy" manifolds which are also part of the attractor but include gravity waves. All manifolds are tangent to the Rossby manifold at the origin. Further, it is possible that the slow manifold is unstable, at least for higher values of the forcing, and consequently, gravity wave-containing manifolds may be more stable and attractive.

Our version of the attractor is based, in part, on the extensive analysis available of the Lorenz attractor (first presented by Lorenz in his seminal 1963 article). In the monograph of Sparrow (1982) it is pointed out that the original Lorenz attractor contains an infinite number of unstable periodic cycles. By analogy, we expect that the present model must contain an infinite number of unstable periodic orbits too. However, a fundamental difference between the 1963 model and the current one is that the periodic cycles are not only unstable but, for a range of parameter values, also exhibit gravity wave oscillations.

We also note that the recent work of Jacobs (1991) demonstrates the existence of the slow manifold for a 5-variable system. In that case, it is unclear as to whether this manifold could be globally slow and globally invariant for the same parameter regime (Lorenz, 1992). Camassa (1994) and Boyd (1994a) demonstrate that this five equation system cannot have a truly slow globally invariant manifold. In contrast, our work only addresses the original nine equation presented in Lorenz (1980). We offer evidence suggesting that a locally invariant manifold exists in that model for low forcing values.

6. Acknowledgements

This work benefitted from discussions with Drs. P. Gent, J. McWilliams, and J. Tribbia, as well as useful comments from Geoffrey Vallis and two anonymous reviewers. The research of JHC and MNL was supported, in part, by National Science Foundation grant ATM-85-19947. SEH was supported by NSF under grant ATM-90-11413 and also thanks the National Center for Atmospheric Research, partially funded by the National Science Foundation, for sponsoring her as a visiting scientist during this work. The majority of the calculations were performed on the CYBER-205 at the John von Neumann Center in Princeton, New Jersey and some have been carried out on the Cray YMP-8/864 at NCAR. We particularly wish to thank Suzanne Whitman for drawing the schematics.

7. Appendix A

Application of the Newton Kantorovich Theorem

The Newton-Kantorovich theorem is a powerful tool. If the hypotheses of the theorem (stated below) are satisfied, it then guarantees that a unique solution to the iteration exists within a ball surrounding the initial guess. The discussion here follows Rall (1969), section 22. Specifically, the equation

$$P(x)=0 \tag{A1}$$

can be solved using the Newton-Kantorovich iteration

$$x_{m+1}=x_m-[P'(x_m)]^{-1}P(x_m),\quad m=1,2,3,\ldots, \tag{A2}$$

provided the following conditions are satisfied:

(a) $\|P''(x)\|\leqslant K$ in some closed ball $\bar{U}(x_0, r)$, (A3a)

(b) $\|[P'(x_0)]^{-1}\|\leqslant B_0$, (A3b)

(c) $\|x_1-x_0\|\leqslant \eta_0$. (A3c)

If these hypotheses are satisfied then there is a unique solution x^* in a ball of radius r_0, $\bar{U}(x_0, r_0)$, with

$$r_0=\frac{1+\sqrt{1-2h_0}}{h_0}\eta_0 \tag{A4}$$

for $h_0=B_0\eta_0K\leqslant\frac{1}{2}$. The difficulty lies in computing the bounds K, B_0, and η_0. When applied to (6), the bounds of (A3b) and (A3c) can be readily estimated. It is more difficult to determine the bound on the second derivative, the so-called "Lipschitz" condition indicated in (A3a). We approximate that bound numerically by spanning the space and checking only isolated points. To do this, a small ε is added and subtracted in each of 6 directions, thus checking points on the boundary and at the vertices of a cube with side length 2ε in $\Re^6$. We then increase ε to determine the largest possible cube in which the hypotheses would be satisfied. There is no loss of generality by considering cubes since topologies generated by norms in finite dimensional Banach spaces are equivalent.

This method is depicted schematically in Fig. 8. Here we see that each ball (projected onto a two dimensional plane) is nested within the ball from the previous iteration. As the iteration proceeds, the radii of the balls decrease and the x_i converge toward x_*.

REFERENCES

Allen, J. S., Barth, J. A. and Newberger, P. A. 1990a. On intermediate models for barotropic continental shelf and slope flow fields. Part I: Formulation and comparison of exact solutions. *J. Phys. Oceanog.* **20**, 1017–1042.

Allen, J. S., Barth, J. A. and Newberger, P. A. 1990b. On intermediate models for barotropic continental shelf and slope flow fields. Part III: Comparison of numerical model solutions in periodic channels. *J. Phys. Oceanog.* **20**, 1949–1973.

Baer, F. and Tribbia, J. J. 1977. On complete filtering of gravity modes through nonlinear initialization. *Monthly Weather Rev.* **105**, 1536–1539.

Barth, J. A., Allen, J. S. and Newberger, P. A. 1990. On intermediate models for barotropic continental shelf and slope flow fields. Part II: Comparison of numerical model solutions in doubly periodic domains. *J. Phys. Oceanog.* **20**, 1044–1076.

Bartle, R. G. and Sherbert, D. R. 1982. *The elements of real analyses.* John Wiley and Sons, 370 pp.

Boyd, J. P. 1994a. Eight definitions of the slow manifold: Seiches, pseudoseiches, and exponential smallness. *Dyn. Atmos. Oceans*, in press.

Boyd, J. P. 1994b. The slow manifold of a five-mode model. *J. Atmos. Sci.* **51**, 1057–1064.

Camassa, R. 1994. On the geometry of a slow manifold. *Physica D*, in press.

Curry, J. H. and Winsand, D. 1986. Low-order intermediate models: bifurcation, recurrence, and solvability. *J. Atmos. Sci.* **43**, 2360–2373.

Daley, R. 1991. *Atmospheric data analysis.* Cambridge University Press, 457 pp.

Daley, R. 1981. Normal mode initialization. *Reviews of Geophys. and Space Phys.* **19**, 450–468.

Errico, R. M. 1982. Normal mode initialization and the generation of gravity waves by quasi-geostrophic forcing. *J. Atmos. Sci.* **39**, 573–586.

Errico, R. M. 1984. The statistical equilibrium solution of a primitive-equation model. *Tellus* **36A**, 42–51.

Errico, R. M. 1989. *Theory and application of nonlinear normal mode initialization.* NCAR Technical Note NCAR/TN-344 + IA, National Center for Atmospheric Research, Boulder, Co, 137 pp.

Gent, P. R. and McWilliams, J. C. 1982. Intermediate model solutions to the Lorenz equations: Strange attractors and other phenomena. *J. Atmos. Sci.* **39**, 3–13.

Gent, P. R. and McWilliams, J. C. 1983a. Consistent balanced models in bounded and periodic domains. *Dyn. Atmos. Oceans* **7**, 67–93.

Gent, P. R. and McWilliams, J. C. 1983b. Regimes of validity for balanced models. *Dyn. Atmos. Oceans* **7**, 167–183.

Guckenheimer, J. and Holmes, P. 1983. *Nonlinear oscillations, dynamical systems, and bifurcations of vector fields.* Springer-Verlag, 453 pp.

Jacobs, S. J. 1991. On the existence of a slow manifold in a model system of equations. *J. Atmos. Sci.* **48**, 793–801.

Kopell, N. 1985. Invariant manifolds and the initialization problem for some atmospheric equations. *Physica* **14D**, 203–215.

Krishnamurthy, V. 1985. *The slow manifold and the persisting gravity waves.* PhD thesis, Massachusetts Institute of Technology, 146 pp.

Leith, C. E. 1980. Nonlinear normal mode initialization and quasi-geostrophic theory. *J. Atmos. Sci.* **37**, 958–968.

Lorenz, E. N. 1960. Maximum simplification of the dynamic equations. *Tellus* **12**, 243–254.

Lorenz, E. N. 1963. Deterministic nonperiodic flow. *J. Atmos. Sci.* **20**, 130–141.

Lorenz, E. N. 1980. Attractor sets and quasi-geostrophic equilibrium. *J. Atmos. Sci.* **37**, 1685–1699.

Lorenz, E. N. 1982. Low-order models of the atmospheric circulations. *J. Meteorol. Soc. Japan* **60**, 255–267.

Lorenz, E. N. 1986. On the existence of a slow manifold. *J. Atmos. Sci.* **43**, 1547–1557.

Lorenz, E. N. and Krishnamurthy, V. 1987. On the nonexistence of a slow manifold. *J. Atmos. Sci.* **44**, 2940–2950.

Lorenz, E. N. 1992. The slow manifold. What is it? *J. Atmos. Sci.* **49**, 2449–2451.

Machenhauer, B. 1977. On the dynamics of gravity wave oscillations in a shallow water model with application to normal mode initialization. *Beitr. Phys. Atmos.* **50**, 253–271.

McWilliams, J. C. and Gent, P. R. 1980. Intermediate models of planetary circulations in the atmosphere and ocean. *J. Atmos. Sci.* **37**, 1657–1678.

McWilliams, J. C., Gent, P. R. and Norton, N. J. 1986. The evolution of balanced, low-mode vortices on the β-plane. *J. Phys. Oceanog.* **16**, 838–855.

McWilliams, J. C., Norton, N. J., Gent, P. R. and Haidvogel, D. B. 1990. A linear balance model of wind-driven, midlatitude ocean circulation. *J. Phys. Oceanog.* **20**, 1349–1378.

Norton, N. J., McWilliams, J. C. and Gent, P. R. 1986. A numerical model of the balance equations in a periodic domain and an example of balanced turbulence. *J. Comp. Phys.* **67**, 439–471.

Rall, L. B. 1969. *Computational solution of nonlinear operator equations.* Wiley and Sons, NY, 225 pp.

Spall, M. A. and McWilliams, J. C. 1991. Rotational and gravitational influences on the degree of balance in the shallow water equations. *Geophys. Astrophys. Fluid Dynamics* **64**, 1–29.

Sparrow, C. 1982. *The Lorenz equations: bifurcations, chaos, and strange attractors.* Springer-Verlag, 269 pp.

Stoer, J. and Bulirsch, R. 1980. *Introduction to numerical analysis.* Springer-Verlag, NY, 609 pp.

Sundermeyer, M. A. and Vallis, G. K. 1993. Correlation dimensions of primitive equation and balanced models. *J. Atmos. Sci.* **50**, 2556–2564.

Vallis, G. K. 1992. Mechanisms and parameterizations of geostrophic adjustment and a variational approach to balanced flow. *J. Atmos. Sci.* **49**, 1144–1160.

Vautard, R. and Legras, B. 1986. Invariant manifolds, quasi-geostrophy, and initialization. *J. Atmos. Sci.* **43**, 565–584.

Warn, T. and Menard, R. 1986. Nonlinear balance and gravity-inertial wave saturation in a simple atmospheric model. *Tellus* **38A**, 285–294.